Vol. 20, No. 1 (2021) 509-519
Revista Mexicana de Ingeniería Química

Application of FESEM and FTIR for evaluation of *Staphylococcus aureus* biofilms grown on chitin and polycarbonate membrane

Aplicación de FESEM y FTIR para la evaluación de biopelículas de *Staphylococcus aureus* cultivadas en membranas de quitina y policarbonato

R. Baishya[1], R. Chatterjee[2], S. Banerjee[1]* and M. S. Hasnain[3]

[1]*Department of Biotechnology, Heritage Institute of Technology, Kolkata 700107, India.*
[2]*Department of Hotel Management and Catering Technology, Birla Institute of Technology, Mesra, Ranchi 835215, India.*
[3]*Department of Pharmacy, Shri Venkateshwara University, Gajraula, Uttar Pradesh 244236, India.*

Received: October 10, 2020; Accepted: December 17, 2020

Abstract

The aim of this study was to use Field Emission Scanning Electron (FESEM) and Fourier transform infrared spectroscopy (FTIR), to investigate the structure and the film-forming capacity of *Staphylococcus aureus*, on two different surface materials, Chitin and Polycarbonate membrane filter. Both the substrates, having diverse properties, showed varied attachments of bacterial and biofilm development. FESEM showed that higher bacterial colonization and biofilm growth was obtained in the rough surface of chitin with complex structure, compared to that of polycarbonate membrane at different time intervals. Due to its high magnification and resolution, FESEM enabled a more detailed analysis of the biofilm cells, influenced by different structural organisations and morphology. On the other hand, FTIR analyses revealed the chemical conformation of the substrate and its biofilm state. However, the difference in the spectra of the two substrates was not large. Prominent band absorbance at 1200-800 cm^{-1} for polysaccharides and proteins at 1700- 1400 cm^{-1} were observed at its biofilm states. These findings promote the prospect of using FESEM and FTIR for understanding biofilm morphology and architecture, as well as its chemical interaction with the substrate.

Keywords: Field Emission Scanning Electron (FESEM); fourier transform infrared spectroscopy (FT-IR); biofilm; chitin; polycarbonate membrane filter; *Staphylococcus aureus*.

Resumen

El objetivo de este estudio fue utilizar Field Emission Scanning Electron (FESEM) y espectroscopia infrarroja por transformada de Fourier (FTIR), para investigar la estructura y la capacidad de formación de película de *Staphylococcus aureus*, en dos materiales de superficie diferentes, quitina y filtro de membrana de policarbonato. Ambos sustratos, que tienen diversas propiedades, mostraron diversas uniones de desarrollo de bacterias y biopelículas. FESEM mostró que se obtuvo una mayor colonización bacteriana y crecimiento de biopelículas en la superficie rugosa de la quitina con estructura compleja, en comparación con la de la membrana de policarbonato en diferentes intervalos de tiempo. Gracias a su gran aumento y resolución, FESEM permitió un análisis más detallado de las células del biofilm, influenciadas por diferentes organizaciones estructurales y morfológicas. Por otro lado, los análisis FTIR revelaron la conformación química del sustrato y su estado de biopelícula. Sin embargo, la diferencia en los espectros de los dos sustratos no fuegrande. Se observó una absorbancia de banda prominente a 1200-800 cm^{-1} para polisacáridos y proteínas a 1700-1400 cm^{-1} en sus estados de biopelícula. Estos hallazgos promueven la posibilidad de utilizar FESEM y FTIR para comprender la morfología y la arquitectura de la biopelícula, así como su interacción química con el sustrato.

Palabras clave: Electrón de barrido de emisión de campo (FESEM); espectroscopía infrarroja por transformada de Fourier (FT-IR); biofilm; quitina; filtro de membrana de policarbonato; *Staphylococcus aureus*.

* *Corresponding author. E-mail*: somabanerjee2005@gmail.com
Tel. 009831074344
https://doi.org/10.24275/rmiq/Poly2118
ISSN:1665-2738, *issn-e*: 2395-8472

1 Introduction

Since last few decades, a variety of natural and synthetic biomaterials have been used for many biomedical applications (Hasnain *et al*., 2017a; 2019a; Nayak and Hasnain, 2019a). These engineered biomaterials includes polymer-blends (Sinha *et al*., 2015), gels (Hasnain *et al*., 2020a), hydrogels (Kurakula *et al*., 2020; Nayak *et al*., 2020), particulates (beads, microparticles, nanoparticles, etc) (Hasnain *et al*., 2018a; Nayak and Hasnain, 2019b), composites and nanocomposites (Hasnain *et al*., 2019b), scaffolds (Nayak *et al*., 2020), membranes and films (Hasnain *et al*., 2020b), pastes (Hasnain *et al*., 2018b), etc., for a variety of important biomedical uses. Nowadays, there is an increasing fashion for the use of naturally-derived biopolymers like chitin and chitosan (Hasnain and Nayak, 2018), alginates (Kurakula *et al*., 2020), gellan gum (Milivojevic *et al*., 2020), etc., in biomedical applications. Amongst these, chitin is being used in many biomedical fields including antimicrobial applications (Brunner *et al*., 2009; Banerjee *et al*., 2015; Fernández-Delgado *et al*., 2015). Biofilm treatment and control in dwelling medical devices and implants, still is a great challenge, as the bacterial colonization is embedded in a self-secreted matrix of extracellular polymeric substances (EPS), making it resistant to antibiotic treatments. Both Gram-positive and Gram-negative bacteria can cause biofilm-associated infections that represent 80% of nosocomial infections of which *Staphylococcus aureus* is the foremost species (Reffuveille *et al*., 2017). In order to treat biofilm efficiently, a detailed understanding is required about its interaction with the cells, the surface of the substrate and its mechanism against the antibiotics (Costerton and Stewart, 2001). The substrate materials, its origin, organic or inorganic surfaces play an important role in bacterial adhesion, growth of biofilms and even in biofilm architecture (Azevedo, 2006).

Recent development in microscopic imaging techniques has helped researchers gain knowledge about biofilms and their structural morphology, among which confocal laser scanning microscopy (CLSM), Scanning electron microscopy (SEM), Standard optical microscopy, epifluorescence microscopy (EM) are the most commonly used. SEM is an appropriate tool with higher magnification and resolution, necessary to observe the shape and organization of the micro-organism forming biofilms (Norton *et al*., 1998; Hannig *et al*., 2010). The detail morphology of the substrate on which the biofilms have adhered along with the bacterial irreversible adhesion, can be followed in the SEM analysis of medical devices (Raad *et al*., 1993; Stickler *et al*., 1998). For analysis and characterization of biofilms on medical devices, SEM has been an effective tool and is currently being used to study the development of antibiofilm constituents against biofilm pathogens (Grenho *et al*.,2014; Sevinc *et al*., 2010; Steffensen *et al*., 2015). When a solid substrate is exposed to an in-vitro environment, it absorbs the dissolved nutrients and the organic matter present in the system, mimicking implanted biomaterials absorbing biological fluids (viz. plasma, blood, urine) (Huang *et al*., 2000; Rios *et al*., 2007). Due to this absorption, the substrate changes its characteristics and physical properties i.e. hydrophobicity, surface charges and roughness (Hetrick and Schoenfisch, 2006). Researchers have found that the changed substrate properties, nutrient accessibility and hydrodynamics, affect the architecture of biofilm (Stoodley, 1997). Moreover, the substrate material, its origin, organic and inorganic surfaces, also plays an important role in bacterial adhesion and in the growth of biofilms (Azevedo, 2006).

Fourier transform infrared spectroscopy (FTIR) is an effective analytical tool based on the vibration of atoms, functional groups, and chemical bonds within the molecules. FTIR analyse the chemical conformation of biological samples by absorbing the mid IR radiation and transforming it into vibrational motion (Hong *et al*., 1999). The biological components absorb different frequencies of light as they differ from each other in the bond type and give a specific absorption pattern at 800-4000 cm^{-1} (Goodacre *et al*., 2000). FTIR spectra are precise with long-term constancy, reproducibility, and the ability to measure even insignificant differences in the configuration of biological constituents and can thus be used as a base for classification and discrimination (Huang *et al*., 2006). Bacterial FTIR spectra show the characteristics of cell components, such as nucleic acids, lipids, carbohydrates, membrane and intracellular proteins, and polysaccharides (Bosch *et al*., 2006).

Previous researcher had shown the importance of FTIR and FESEM analysis of gram negative bacteria like *Pseudomonas aeruginosa* biofilm on different substrate (Singh *et al*., 2017). This study shows use of FTIR and Field Emission Scanning electron microscopy (FESEM), to compare the adhesion and

architecture of biofilm formation by *Staphylococcus aureus* strains on two different surface chitin flakes (a natural aminopolysaccharide polymer) and polycarbonate membrane filter (synthetic biomaterial). The FTIR spectra and the high-resolution micrographs provide vital information on the surface-biofilm interaction, cell colonization and its morphological changes.

The main aim of the study was to understand the substrate-microbes interaction on both the attached surfaces with the two different techniques FESEM and FTIR, both having different analytical approaches. The novelty of the manuscript mainly lies on the biofilm architecture pattern adherence which changes according to the substrate.

2 Materials and methods

2.1 Bacterial strains and growth conditions

Experiments were performed with *Staphylococcus aureus* ATCC 25923, maintained in Tryptic soya agar (TSA). A single colony of the organism was inoculated into Trypticase soya broth (TSB) medium and incubated at 37ºC for 24 hours (hrs) under appropriate aerobic conditions before each experiment.

2.2 Biofilm formation in vitro on Chitin flakes as substrate

Trypticase soya broth (TSB) medium was inoculated with *Staphylococcus aureus* ATCC 25923 culture from Tryptic Soya Agar (TSA) slant and incubated at 37 ºC overnight to yield a concentration of 1×10^6 CFU/ml. Flask with 100 ml of TSB with 0.3% of chitin flakes (Himedia, India) were then inoculated with 1ml aliquot of the cells and was incubated at 37 ºC for 24 hrs and 72 hrs for the establishment of biofilm in the substrate i.e. chitin flakes (Banerjee *et al.*, 2015).

2.3 Biofilm formation in vitro on polycarbonate membrane filter as substrate

The biofilms of *S. aureus* ATCC 25923 were grown on white, polycarbonate membranes (PMF) (Merck Millipore, India) according to the method of Anderl *et al.*, (2000) with modifications. A 100 μL of culture was used to seed the polycarbonate membranes (diameter, 13 mm; pore size, 0.4 μm) placed on tryptic soy agar plates. The plates were inverted and incubated at 37 ºC for 24 hrs and 72 hrs, with the membrane-supported biofilms transferred to fresh culture medium every 24 hrs.

2.4 Biofilm observation by FESEM and FTIR

After each incubation time, the substrate from each culture was removed, rinsed three times with phosphate-buffered saline (PBS, pH 7.4), treated with glutaraldehyde, and dried until the FESEM analysis (Sigma 300 Model, Zeiss make). Duplicate samples of substrates cultured with *S. aureus* strain were analysed using FESEM, for which the surface of each sample was chosen randomly to obtain representative images over the biofilm formation. Frequencies of the different biofilms structures formed in both the substrates were compared to the control (without biofilm) surface. The FTIR spectra were recorded in the range of 4000-500 cm^{-1}, using a spectrometer (Shimadzu make). Two replicates were taken for each sample. The spectra were processed using an IR solution Software Overview (Shimadzu) and Origin 8 SR1 Software. 2.1.

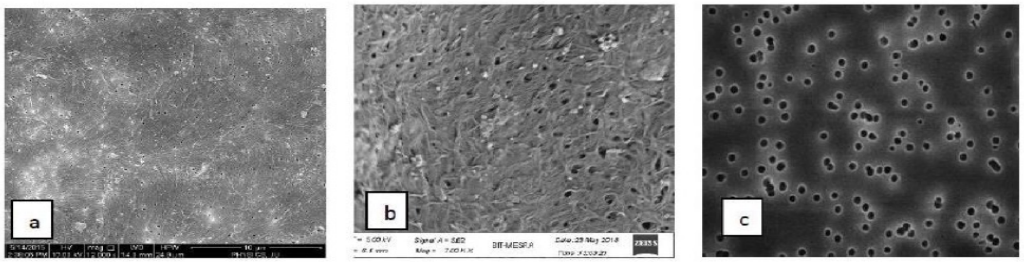

Fig. 1. Representative FESEM images of surface tested without *S. aureus* biofilm chitin at 1200X (a) chitin at 7000X (b) and polycarbonate membrane filter at 10000X (c). (Scale bar 5-10 μm).

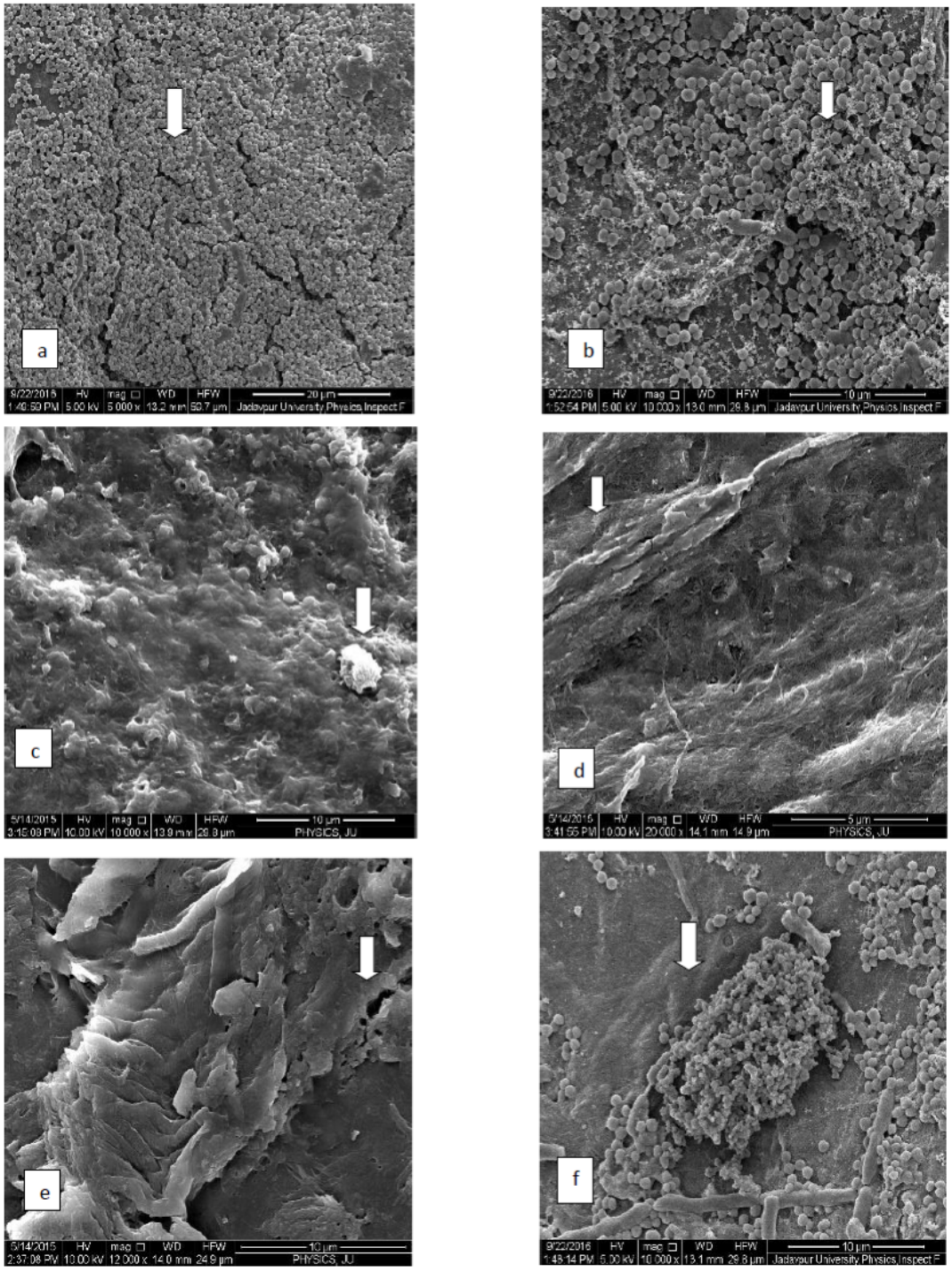

Fig. 2. Representative FESEM images of *S. aureus* biofilms formed on chitin flakes at 24 hrs (a) and at 72 hrs (b-f) showing increase in biofilm formation. Layer of single cell colonisation with small crystal like deposition seen at 24 hrs (a). At 72 hrs, distinct EPS layer (b) observed with matured and organised structures of biofilm like honeycombs (c), walls (d), channels (e) and mushroom like structures (f). Down arrows indicate each structure in each image. (Scale bar 5-10 μm).

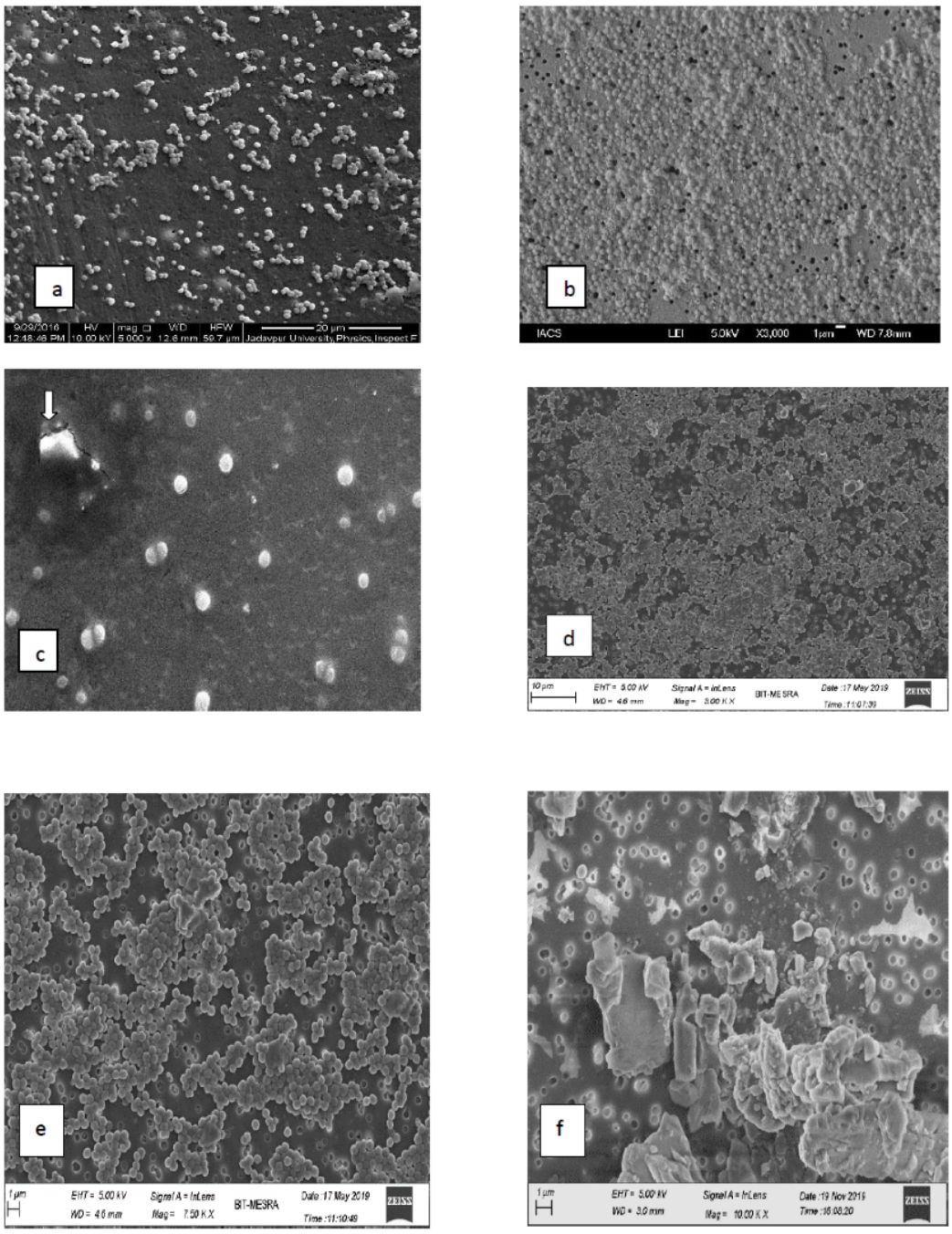

Fig. 3. Representative FESEM images of *S. aureus* biofilms formed on polycarbonate membrane at 24 hrs (a) and at 72 hrs (b) with few channels (c). Down arrow indicates in Fig 3(c). Chitin flakes with no complex architecture of biofilm at 72 hrs (Figure 3d, 3e). EPS formation at 72 hrs (Figure 3f). (Scale bar 5-10 μm).

3 Results

3.1 Biofilm formation of S. aureus evaluated by FESEM

S. aureus biofilms formed on chitin and polycarbonate membrane surfaces showed a difference in growth pattern in both the surfaces with respect to time (24 and 72 hrs) when analysed by FESEM. Figure 1 represents the two tested surfaces without bacterial inoculation (control). Chitin flakes were found to have a heterogeneous and rough surface (Figure 1a and 1b) while polycarbonate membranes were smooth and homogeneous, porous membrane (Figure 1c). It was observed that after 24 hrs the biofilm attached to the chitin formed a monolayer colony of the cells with some crystal-like depositions attached to the surface and to the bacterial cells (Figure 2a, Figure 2b). After 72 hrs, the chitin flakes showed highly organised structures of biofilm with extracellular matrix production. During the period from 24 to 72 hrs the organised structures were evident on the chitin flakes.

Few specialised structures like honeycombs, and walls were seen during the 72 hrs biofilm formation (Figure 2c, Figure 2d respectively) along with channels (Figure 2e) and mushroom like structures (Figure 2f) embedded within them with a distinct cellular growth.

In polycarbonate membrane, bacterial attachment appeared less at 24 hrs (Figure 3a) with no EPS formation. However, at 72 hrs single layer colonies (Figure 3b) of *S. aureus* biofilm were observed with few channels (Figure 3c) at some areas. However, unlike in chitin flakes no complex architecture of biofilm was observed at 72 hrs (Figure 3d, 3e). EPS formation was seen in few PMF at 72 hrs (Figure 3f). Numbers of channels observed within the polycarbonate membrane biofilm were much less when compared with their high frequency in the chitin biofilms. At the same time matured EPS and any other highly organised structured were absent.

3.2 Biofilm formation of S. aureus evaluated by FTIR

FTIR data showed the presence of bacteria within the biofilm, showing presence of nucleic acids. It is evident that the EPS matrices formed by the bacterial strains, produced differences in the chitin flakes regarding their chemical composition and chemical constituents, in respect to the embedded biofilm. Characteristic marker of CH deformation of the β-glycosidic bond was observed at 890cm^{-1} to 895 cm^{-1} in chitin, with two additional bands for CHx deformations at about 1455 and 1374 cm^{-1} (Brunner *et al.*, 2009). The IR spectral region at around 1700-1600 cm^{-1} is assigned to the peptide backbone of amide I and 1600-1500 cm^{-1} for amide II absorption. However, the absorptions at 1648-1554 cm^{-1} and 1535-1542 cm^{-1} were for random coil structure (Xiong *et al.*, 2019; Lu *et al.*, 2010).

Spectra of chitin showed several standard narrower bands in the C-O-C and C-O stretching vibration region (1200-950 cm^{-1}). In the region between 1700 and 1500 cm^{-1} the C=O stretching region of the amide moiety was present. The amide I bands showed different components at 1660 to 1630 cm^{-1} either because of hydrogen bonding or due to enol presence in the moiety. The amide II band was observed at 1558-1562 cm^{-1}.

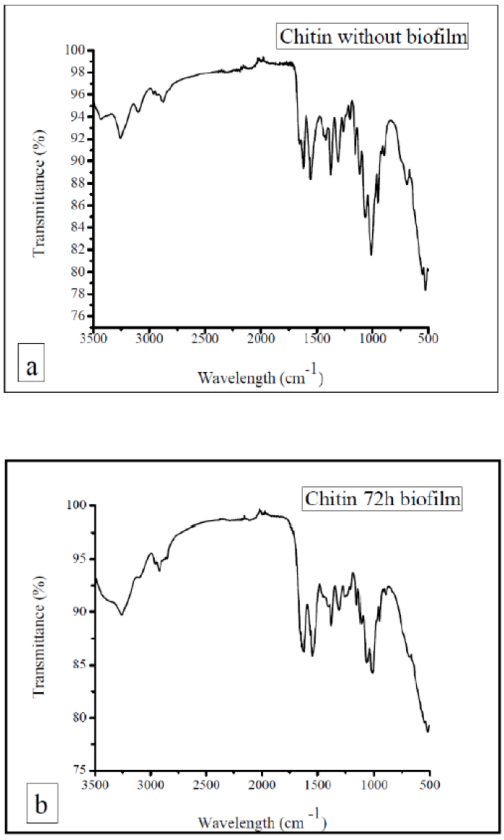

Fig. 4. FTIR of chitin control (a) and with biofilm formation at 72 hrs (b) at range 500-3500 cm^{-1}.

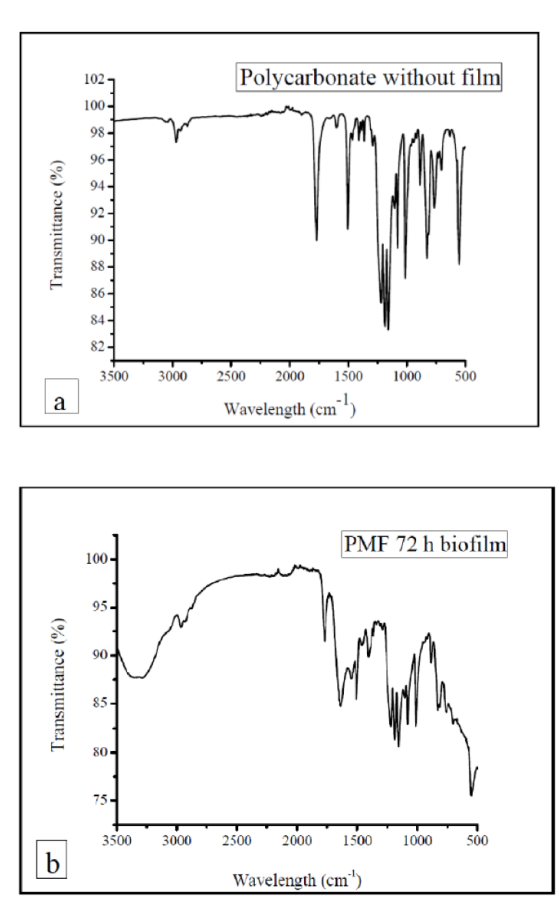

Fig. 5. FTIR of polycarbonate membrane filter control (a) and with biofilm formation at 72 hrs (b) at range 500-3500 cm^{-1}.

The FTIR spectral of chitin also showed presence of the following bands of -NH_2, -OH at 3390-3418 cm^{-1}; the C-H stretching band at 2870-2880 cm^{-1}; C3-OH at 1178-1189 cm^{-1} and 1148-1153 cm^{-1} and C6-OH at 1073-1074 cm^{-1} (Figure 4a). FTIR spectra of chitin with biofilm, differs from the control spectra, both in shape and in the transmittance intensity within the same range of wave number, due to the variation in the conformation and amount of each component. The spectra indicate the presence of polysaccharides and nucleic acids in the exopolysaccharide matrix of the biofilm (1200-800 cm^{-1}), proteins at 1700- 1400 cm^{-1} and peaks for lipids (2830 - 3250 cm^{-1}) (Figure 4b).

In polycarbonate membrane filter like chitin, several FTIR spectra (Figure 4a) peaks were observed at 800 cm^{-1}, 1024 cm^{-1}, 1250 cm^{-1} and 1272 cm^{-1} due to C-O bond stretching. C-H vibrations were observed at 1380 cm^{-1}. At 1500 -1630 cm^{-1}, peaks were observed due to C=C bonds of the aromatic carbon ring, and C=O bonds peaks at1760 cm^{-1}. It can be concluded from Figure 5(a) that for C- H band, peaks appear at 2850- 2970 cm^{-1}. In the fingerprint range 500- 1000 cm^{-1}, peak was mainly for C-C bond stretching. A similar difference was observed in the spectra with 72 hrs biofilm in polycarbonate membrane (Figure 4b), as in the biofilm formation in chitin. The peaks showed intensity variation in the same range of the spectra, conforming addition of polysaccharides and proteins in the substrate, with wide band ranges. However, the bands of the two-substrates showed intensity difference in the peaks with well-defined smooth and sharp peaks in polycarbonate membrane.

4 Discussion

In the present study, we evaluated and compared the biofilm formation of *S. aureus* strain, using two different substrate systems: chitin and polycarbonate membrane. Initially, the architecture of the biofilms formed on both the substrates, were studied in their native states. The use of FESEM in this study showed that the strain was able to form diverse biofilm structures on chitin and polycarbonate membranes. Chitin contained larger number of adhered cells and aggregates which formed rapid biofilm architecture from 24 to 72 hrs (Figure 2), as compared to polycarbonate membranes, which had a much slower growth of biofilm.

The biofilm formed on chitin showed complex and high ordered structures like channels, honeycombs, walls, and mushroom like structures in a well-defined EPS matrix. Such complex structures of biofilm have been observed in mature biofilms of clinical strains of P. mirabilis at 24-96 hrs, in the study of Fernández-Delgado *et al*. (2015). Stoodley *et al*. (2002) in their study showed that bacterial biofilm varies in their responses to environmental conditions such as nutrient limitation, shear, flowrate, and pressure. In chitin, structures like mushrooms and honeycombs were seen to be surrounded by walls and channels which might be due to the need to increase the nutrients flow inside the biofilm association, in order to survive in the exposed environmental conditions. Pruzzo *et al*. (2008) described attachment of *Vibrio cholera* to chitin and the role of surface proteins in its association, with chitinous fauna, availability of food, adaptation

to environmental nutrient, stress tolerance, and most importantly, its protection from lethal compounds. Similarly, biofilm formed on chitin flakes by *S. aureus* in the present study, may have developed an ability to attach to chitin. The surface roughness and proteins of chitin also influence bacterial attachment and biofilm growth, in contrast to biofilm formed on polycarbonate membrane filter, where only flat layer biofilms could be observed between 24 and 72 hrs (Figure 3).

The chemical structure of chitin by FTIR was discussed by Brunner *et al*. (2009). Spectra of chitin were observed in the present study, with peaks at different band ranges, conforming the presence of different chemical bonds and interactions. However, the peaks of both the substrate spectra showed little/no difference, except variations in their peak intensities. The presence of the bacterial biofilm was revealed through FTIR data (Figure 4 & 5), showing presence of nucleic acids and polysaccharides (Jiao *et al*., 2010). FTIR spectra of EPS matrix of the individual substrate demonstrated contrasts between them due to their chemical compositions and constituents.

The stronger band intensities and peak areas in the biofilm spectra could be due to the distinctions in metabolic states and maturing of the cells over the span of biofilm arrangement (Geesey and Uhite, 1990). Delille *et al*. (2007) reported the intensity of amide II band, which increased with time because of biomass aggregation, thus increasing the surface area by the bacteria. Indeed, when bacteria appends to a surface, significant physiological changes upgrade their metabolic activity, resulting in increased area in the biofilm spectra (Geesey and Uhite, 1990).These may also be due to the expansion of the complex sugar band found between 1200- 900 cm^{-1} that characterises the additional intracellular polysaccharides (Parolis *et al*., 1991).

The main changes between the samples have been shown in the protein, lipid, and sugar regions. The change in the amide bands are due to the secondary structures of proteins (Barth, 2007). Absorbance bands 1500-1700 cm^{-1} for amide I and amide II are relatively higher in both substrates with biofilm compare to without biofilm substrates.

The characteristic region for sugar 1200-800 cm^{-1} is important for the structural characterization of polysaccharides. The change in the region 750-1250 cm^{-1} indicated the presence of oligosaccharides in biofilm tested samples conforming the presence of exopolysaccharide matrix. The change in the intensities of these regions are higher in chitin flakes compared to PMF.However, due to overlying of water analytical value of FT-IR spectroscopy maybe reduced though bacterial biofilms have dissimilar densities (Sabbatini *et al*., 2017).

In conclusion, this study has reported the ability of *S. aureus* strains to develop distinct biofilms on chitin and polycarbonate membrane. The FESEM analysis however suggests that biofilm formed on chitin were much stronger, thus providing an insight into the current knowledge of *Staphylococcus aureus* biofilm and its attachment to the surface. The chemical structure of the substrate along with the substrate with the biofilm was reported for the first time by FTIR spectroscopy.

Acknowledgements

The authors are thankful to Department of Science and Technology and Biotechnology, West Bengal. India Project No.9G-38 for funding the project. We would like to thank the Central Instrumentation Facility, Birla Institute of Technology, Mesra, Ranchi, India for conducting FESEM and FTIR analysis.

References

Anderl, J. N., Franklin, M. J. and Stewart, P. S. (2000). Role of antibiotic penetration limitation in *Klebsiella pneumoniae* biofilm resistance to ampicillin and ciprofloxacin. *Antimicrobial Agents and Ahemotherapy 44*, 1818-1824.

Aydin Sevinç, B. and Hanley, L. (2010). Antibacterial activity of dental composites containing zinc oxide nanoparticles. *Journal of Biomedical Materials Research Part B: Applied Biomaterials 94*, 22-31.

Azevedo, N. F., Pacheco, A. P., Keevil, C. W. and Vieira, M. J. (2006). Adhesion of water stressed *Helicobacter pylori* to abiotic surfaces. *Journal of Applied Microbiology 101*, 718-724.

Banerjee, S., Saha, A., Dutta, S., Baishya, R. and Maiti, P. K. (2015). Effect of different antibiotics against in vitro *Staphylococcus aureus* biofilm grown on chitin flakes. *South Asian Journal of Experimental Biology 5*, 22-25.

Barth, A. (2007). Infrared spectroscopy of proteins. *Biochimica et Biophysica Acta Bioenergetics 1767*, 1073-1101.

Bosch, A., Golowczyc, M. A., Abraham, A. G., Garrote, G. L., De Antoni, G. L. and Yantorno, O. (2006). Rapid discrimination of lactobacilli isolated from kefir grains by FT-IR spectroscopy. *International Journal of Food Microbiology 111*, 280-287.

Brunner, E., Ehrlich, H., Schupp, P., Hedrich, R., Hunoldt, S., Kammer, M., Machill, S., Paasch, S., Bazhenov, V.V., Kurek, D.V. and Arnold, T. (2009). Chitin-based scaffolds are an integral part of the skeleton of the marine demosponge Ianthella basta. *Journal of Structural Biology 168*, 539-547.

Chu, P. K., Chen, J. Y., Wang, L. P. and Huang, N. (2002). Plasma-surface modification of biomaterials. *Materials Science and Engineering: R: Reports 36*, 143-206.

Costerton, J. W. and Stewart, P. S. (2001). Battling biofilms. *Scientific American 285*, 74-81.

Delille, A., Quiles, F. and Humbert, F. (2007). *In situ* monitoring of the nascent *Pseudomonas fluorescens* biofilm response to variations in the dissolved organic carbon level in low-nutrient water by attenuated total reflectance-Fourier transform infrared spectroscopy. *Applied Environmental Microbiology 73*, 5782-5788.

Fernández-Delgado, M., Duque, Z., Rojas, H., Suárez, P., Contreras, M., García-Amado, M. A. and Alciaturi, C. (2015). Environmental scanning electron microscopy analysis of *Proteus mirabilis* biofilms grown on chitin and stainless steel. *Annals of Microbiology 65*, 1401-1409.

Geesey, G. G. and Whit, D. C. (1990). Determination of bacterial growth and activity at solid-liquid interfaces. *Annual Review of Microbiology 44*, 579-602.

Goodacre, R., Shann, B., Gilbert, R.J., Timmins, E. M., McGovern, A.C., Alsberg, K., Kell, D.B. and Logan, N.A. (2000). The detection of the dipicolinic acid biomarker in bacillus spores using Curie-point pyrolysis mass spectrometry and Fourier transform infrared spectroscopy. *Analytical Chemistry 72*, 119-127.

Grenho, L., Monteiro, F. J. and Ferraz, M. P. (2014). *In vitro* analysis of the antibacterial effect of nanohydroxyapatite-ZnO composites. *Journal of Biomedical Materials Research Part A 102*, 3726-3733.

Hannig, C., Follo, M., Hellwig, E. and Al-Ahmad, A. (2010). Visualization of adherent micro-organisms using different techniques. *Journal of Medical Microbiology 59*, 1-7.

Hasnain, M. S. and Nayak, A. K. (2018). Chitosan as responsive polymer for drug delivery applications. In: *Stimuli Responsive Polymeric Nanocarriers for Drug Delivery Applications*, Volume 1, Pp. 581-605. Woodhead Publishing, Elsevier Inc., United States.

Hasnain, M. S., Rishishwar, P., Ali, S., Alkahtani, S., Tabish, M., Milivojevic, M. and Nayak, A. K. (2020a). Formulation and *ex vivo* skin permeation of lidocaine HCl topical gels using dillenia (*Dillenia indica* L.) fruit gum. *Revista Mexicana de Ingeniería Química 19*, 1465-1476.

Hasnain, M. S., Guru, P. R., Rishishwar, P., Ali, S., Ansari, M. T. and Nayak, A. K. (2020b). Atenolol-releasing buccal patches made of Dillenia indica L. fruit gum: preparation and ex vivo evaluations. *SN Applied Sciences 2*, 57.

Hasnain, M. S., Rishishwar, P. and Ali, S. (2017a). Floating-Bioadhesive matrix tablets of hydralazine HCl made of cashew gum and HPMC K4M. *International Journal of Pharmacy & Pharmaceutical Sciences 9*, 124-129.

Hasnain, M. S., Rishishwar, P. and Ali, S. (2017b). Use of cashew bark exudate gum in the preparation of 4% lidocaine HCl topical gels. *International Journal of Pharmacy & Pharmaceutical Sciences 9*, 146-150.

Hasnain, M. S., Rishishwar, P., Rishishwar, S., Ali, S. and Nayak, A. K. (2018a). Isolation and characterization of *Linum usitatisimum* polysaccharide to prepare mucoadhesive beads of diclofenac sodium. *International Journal of Biological Macromolecules 116*, 162-172.

Hasnain, M. S., Rishishwar, P., Rishishwar, S., Ali, S. and Nayak, A. K. (2018b). Extraction and characterization of cashew tree (*Anacardium occidentale*) gum; use in aceclofenac dental pastes. *International Journal of Biological Macromolecules 116*, 1074-1081.

Hetrick, E. M., Schoenfisch, M. H. (2006). Reducing implant-related infections: active release strategies. *Chemical Society Reviews 35*, 780-789.

Hong, K., Sun, S., Tian, W., Chen, G.Q. and Huang, W. (1999). A rapid method for detecting bacterial PHA in intact cells by FT-IR. *Applied Microbiology Biotechnology 51*, 523-526.

Huang, W. E., Hopper, D., Goodacre, R., Beckmann, M., Singer, A. and Draper, J. (2006). Rapid characterization of microbial biodegradation pathways by FT-IR spectroscopy. *Journal of Microbiological Methods 67*, 273-280.

Huang, Y., Leobandung, W., Foss, A. and Peppas, N. A. (2000). Molecular aspects of muco- and bioadhesion: Tethered structures and site-specific surfaces. *Journal of Controlled Release 65*, 63-71.

Jiao, Y, Cody, G. D., Harding, A. K., Wilmes, P., Schrenk, M., Wheeler, K. E., Banfield, J.F. and Thelen, M. P. (2010). Characterization of extracellular polymeric substances from acidophilic microbial biofilms. *Applied and Environmental Microbiology 76*, 2916-2922.

Kurakula, M., Rao, G. K., Kiran, V., Hasnain, M. S. and Nayak, A. K. (2020). Alginate-based hydrogel systems for drug releasing in wound healing. In: *Alginates in Drug Delivery*, (A.K. Nayak and M.S. Hasnain, eds.), Pp. 323-358. Academic Press, Elsevier Inc., United States.

Lu,Q., Hu, X., Wang, X., Kluge, J.A., Lu, S., Cebe, P. and Kaplan, D.L. (2010). Water-insoluble silk films with silk I structure. *Acta Biomaterialia 6*, 1380-1387.

Milivojevic, M., Pajic-Lijakovic, I., Bugarski, B., Nayak, A. K. and Hasnain, M. S. (2019). Gellan gum in drug delivery applications. In: *Natural Polysaccharides in Drug Delivery and Biomedical Applications*, (M.S. Hasnain and A.K. Nayak, eds.), Pp.145-186. Academic Press, Elsevier Inc., United States.

Nayak, A. K. and Hasnain, M. S. (2019a). *Plant Polysaccharides-Based Multiple-Unit Systems for Oral Drug Delivery*. (A.K. Nayak and M.S. Hasnain, eds.), Springer, Singapore.

Nayak, A. K. and Hasnain, M. S. (2019b). Background: Multiple Units in Oral Drug Delivery. In: *Plant Polysaccharides-Based Multiple-Unit Systems for Oral Drug Delivery*, (A.K. Nayak and M.S. Hasnain, eds.), Pp. 1-17. Springer, Singapore.

Nayak, A. K., Mohanta, B. C., Hasnain, M. S., Hoda, M. N. and Tripathi, G. (2020b). Alginate-based scaffolds for drug delivery in tissue engineering. *Alginates in Drug Delivery*, (A.K. Nayak and M.S. Hasnain, eds.), Pp.359-386. Academic Press, Elsevier Inc., United States.

Norton, T. A., Thompson, R. C., Pope, J, Veltkamp, C. J., Banks, B., Howard, C.V. and Hawkins, S. J. (1998). Using confocal laser scanning microscopy, scanning electron microscopy and phase contrast light microscopy to examine marine biofilms. *Aquatic Microbial Ecology 16*, 199-204.

Parolis, L. A., Parolis, H., Dutton, G. G., Wing, L. and Skura, B, J. (1992).Structure of the glycocalyx polysaccharide of Pseudomonas fragi ATCC 4973. *Carbohydrate Research 216*, 495-504.

Pruzzo, C., Vezzulli, L. and Colwell, R. R. (2008). Global impact of *Vibrio cholerae* interactions with chitin. *Environmental Microbiology 10*, 1400-1410.

Raad, I., Costerton, W., Sabharwal, U., Sadlowski, M., Anaissie, E. and Bodey, G. P. (1993). Ultrastructural analysis of indwelling vascular catheters: a quantitative relationship between luminal colonization and duration of placement. *Journal of Infectious Diseases 168*, 400-407.

Reffuveille, F., Josse, J., Vallé, Q., Mongaret, C. and Gangloff, S.C. (2017). *Staphylococcus aureus* biofilms and their impact on the medical field. In: *The Rise of Virulence and Antibiotic Resistance in Staphylococcus aureus*, Chapter11. IntechOpen.

Rios, P. F., Dodiuk, H., Kenig, S., McCarthy, S. and Dotan, A. (2007). The effect of polymer surface on the wetting and adhesion of liquid systems. *Journal of Adhesion Science and Technology 21*, 227-241.

Sabbatini, S., Conti, C., Orilisi, G. and Giorgini, E. (2017). Infrared spectroscopy as a new tool for

studying single living cells: Is there a niche? *Biomedical Spectroscopy and Imaging 6*, 85-99.

Samanta, A., De, A., Hasnain, M. S., Bera, H. and Nayak, A. K. (2019). Gum odina as pharmaceutical excipient. In: *Natural Polysaccharides in Drug Delivery and Biomedical Applications*, (M.S. Hasnain and A.K. Nayak, eds.), Pp. 327-337. Academic Press, Elsevier Inc., United States.

Sinha, P., Ubaidulla, U., Hasnain, M. S., Nayak, A. K. and Rama, B. (2015). Alginate-okra gum blend beads of diclofenac sodium from aqueous template using $ZnSO_4$ as a cross-linker. *International Journal of Biological Macromolecules 79*, 555-563.

Sinha, S.D., Chatterjee, S., Maiti, P.K., Tarafdar, S. and Moulik, S.P. (2017). Evaluation of the role of substrate and albumin on Pseudomonasaeruginosa biofilm morphology through FESEM and FTIR studieson polymeric biomaterials. *Progress in Biomaterials 6*, 27-38.

Steffensen, S, L., Vestergaard, M. H., Groenning, M., Alm, M., Franzyk, H. and Nielsen, H. M. (2015). Sustained prevention of biofilm formation on a novel silicone matrix suitable for medical devices. *European Journal of Pharmaceutics and Biopharmaceutics 94*, 305-311.

Stickler, D., Morris, N., Moreno, M. C. and Sabbuba, N. (1998), Studies on the formation of crystalline bacterial biofilms on urethral catheters. *European Journal of Clinical Microbiology and Infectious Diseases 17*, 649-652.

Stoodley, P., Boyle, J. D., Dodds, I. and Lappin-Scott, H. M. (1997). *Consensus Model of Biofilm Structure*, Pp.1-9. Cardiff, U.K.

Stoodley, P., Cargo, R., Rupp, C. J, Wilson, S. and Klapper, I. (2002). Biofilm material properties as related to shear-induced deformation and detachment phenomena. *Journal of Industrial Microbiology and Biotechnology 29*, 361-367.

Xiong, P., Jia, Z., Zhou, W., Yan, J., Wang, P., Yuan, W., Li, Y., Cheng, Y., Guan, Z. and Zheng, Y. (2019). Osteogenic and pH stimuli-responsive self-healing coating on biomedical Mg-1Ca alloy. *Acta Biomaterialia 92*, 336-350.